LLNL-PRES-443673

Robust Quantum-Based Interatomic Potentials for Transition Metals

John A. Moriarty
Lawrence Livermore National Laboratory

Atomistic Simulations for Industrial Needs Workshop

NIST Gaithersburg, MD
July 27, 2010

Collaborators: J. N. Glosli, R. Q. Hood, D. A. Orlikowski, P. Söderlind, M. Tang , C. Wu and L. H. Yang (LLNL)

L. Burakovsky (LANL), A. Belonoshko (RIT, Sweden)

This work was performed under the auspices of the U. S. Department of Energy by Lawrence Livermore National Laboratory under contract No. DE-AC52-07NA27344

Outline

- **Quantum-based interatomic potentials**
  - **linking first-principles quantum mechanics to large-scale atomistic simulation via GPT method**
  - **simplified *model* GPT or MGPT for central transition metals**
- **Selected MGPT applications in Ta, Mo and V prototypes**
  - **high-pressure phase transitions**
  - **multiphase equation of state, melt and polymorphism**
  - **dislocations and multiscale modeling of yield strength**
- **Beyond the standard theory: advanced MGPT capabilities**
  - **matrix MGPT: *f*-electrons, non-canonical bands, fast algorithms**
  - ***sp-d* hybridization: series-end transition metals, e.g., Ni**
  - **inclusion of electron temperature: T-dependent potentials**

Bridging the gap from quantum mechanics to large-scale atomistic simulation

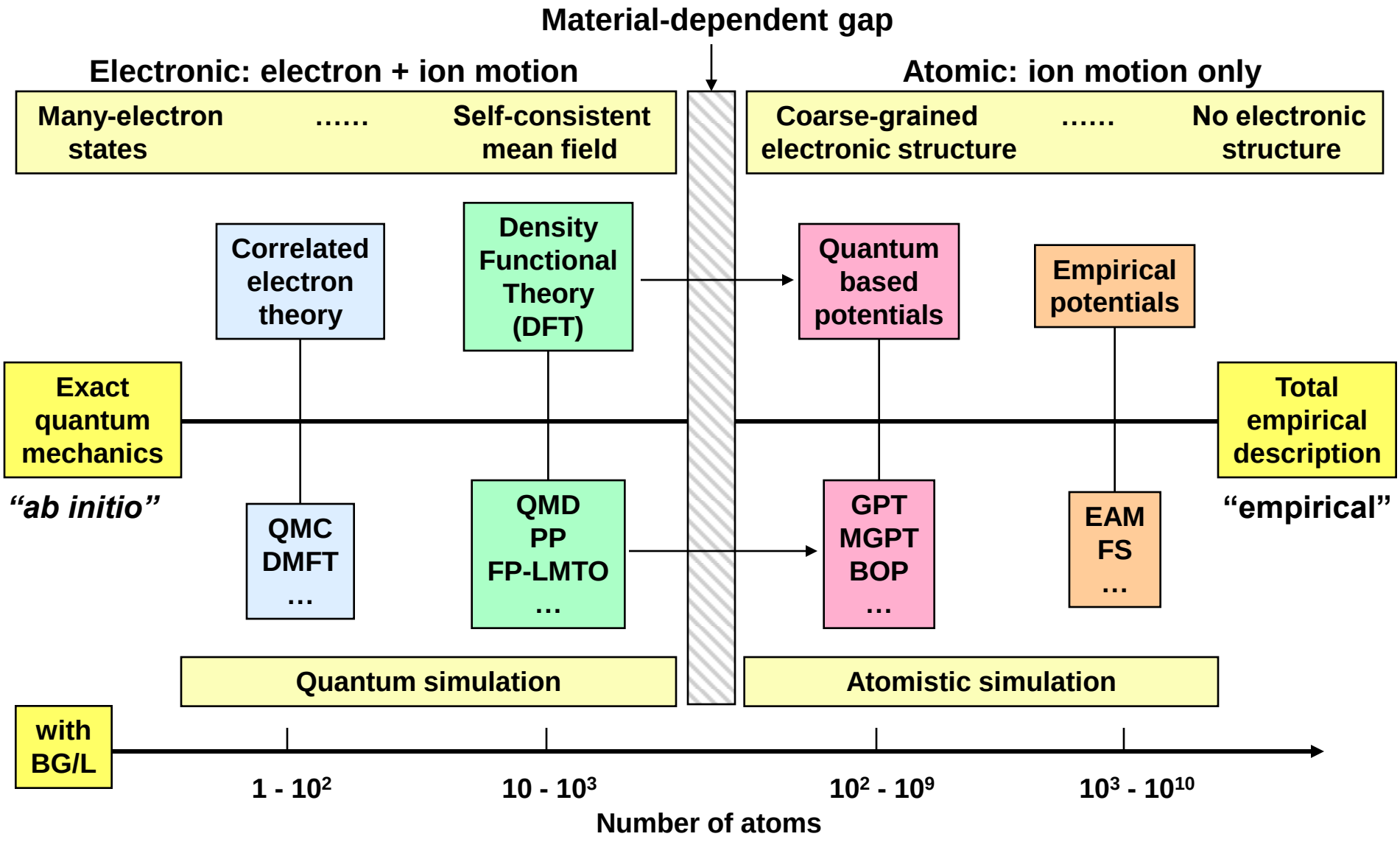

Generalized Pseudopotential Theory (GPT)

- **Mixed basis:** $|\vec{k}>, |\phi_d>$ (DFT quantum mechanics)
  - expansions in weak matrix elements
  - self-consistent screening

sp pseudopotential: $<\vec{k}+\vec{q}\,|\,w\,|\,\vec{k}>$

d-d tight-binding: $<\phi_d^i\,|\,\Delta\,|\,\phi_{d'}^j> \;\&\; <\phi_d^i\,|\,\phi_{d'}^j>$

sp-d hydridization: $<\vec{k}\,|\,\Delta\,|\,\phi_d> \;\&\; <\vec{k}\,|\,\phi_d>$

- **Total-energy functional:** (bulk formulation: atomic volume Ω)

$$E_{tot}(R_1,\ldots,R_N) = NE_{vol}(\Omega) + \frac{1}{2}{\sum_{i,j}}' v_2(ij;\Omega) + \frac{1}{6}{\sum_{i,j,k}}' v_3(ijk;\Omega) + \frac{1}{24}{\sum_{i,j,k,l}}' v_4(ijkl;\Omega)$$

volume radial forces angular forces

  - structure-independent potentials: *rigorous transferability*
  - atomistic simulation: MS, MD, MC

***ab initio* GPT:** simple & series-end transition metals: Mg, Cu, …
binary and ternary alloys: TM_xAl_{1-x} … **GPT**

model GPT: central transition metals: Mo, Ta, …
canonical *d* bands; analytic v_3 and v_4 **MGPT**

Simplified MGPT for central *d*-transition metals

$$E_{tot}(R_1,\ldots,R_N) = NE_{vol}(\Omega) + \frac{1}{2}{\sum_{i,j}}' v_2(ij;\Omega) + \frac{1}{6}{\sum_{i,j,k}}' v_3(ijk;\Omega) + \frac{1}{24}{\sum_{i,j,k,l}}' v_4(ijkl;\Omega)$$

- **Systematic approximations in GPT:**
  - neglect *sp-d* hybridization beyond E_{vol} and fold *d*-state non-orthogonality into v_2
  - introduce canonical *d* bands:

$$\Delta_{dd'}(R_{ij}) \equiv < \phi_d \,|\, \Delta \,|\, \phi_{d'} > = \alpha_m (R_{WS}/R_{ij})^5 \rightarrow \alpha_m (R_{WS}/R_{ij})^p$$

p ~ 4-5 $\quad \alpha_0 : \alpha_1 : \alpha_2$

bcc metals 6: -4: 1

$$v_2(r) = v_2^{sp}(r) + v_2^{hc}(r) + v_a[f(r)]^4 - v_b[f(r)]^2$$

$$v_3(r_1,r_2,r_3) = v_c f(r_1)f(r_2)f(r_3)L(\theta_1,\theta_2,\theta_3) + v_d\{[f(r_1)f(r_2)]^2 P(\theta_3) + [f(r_2)f(r_3)]^2 P(\theta_1) + [f(r_3)f(r_1)]^2 P(\theta_2)\}$$

$$v_4(r_1,r_2,r_3,r_4,r_5,r_6) = v_e[f(r_1)f(r_2)f(r_3)f(r_4)M(\theta_1,\theta_2,\theta_3,\theta_4,\theta_5,\theta_6) + f(r_3)f(r_2)f(r_6)f(r_5)M(\theta_7,\theta_8,\theta_9,\theta_{10},\theta_5,\theta_{12}) + f(r_1)f(r_6)f(r_4)f(r_3)M(\theta_{11},\theta_{12},\theta_5,\theta_6,\theta_3,\theta_4)]$$

$$f(r) \equiv (1.8R_{WS}/r)^p$$

L, P, M universal angular functions (*d* symmetry)

Advanced-generation MGPT potentials: Ta, Mo, V

- **Parameter constraints:** bcc DFT and/or experimental data as a function of Ω

$-E_{vol}$: E_{coh}	$-v_a$: C_{44}	$-v_b$: E^0_{vac}	compressibility sum rule reduces
$-v_d$: B	$-v_e$: C'	$-v_c$: Θ_D	independent parameters to 5

Two-ion

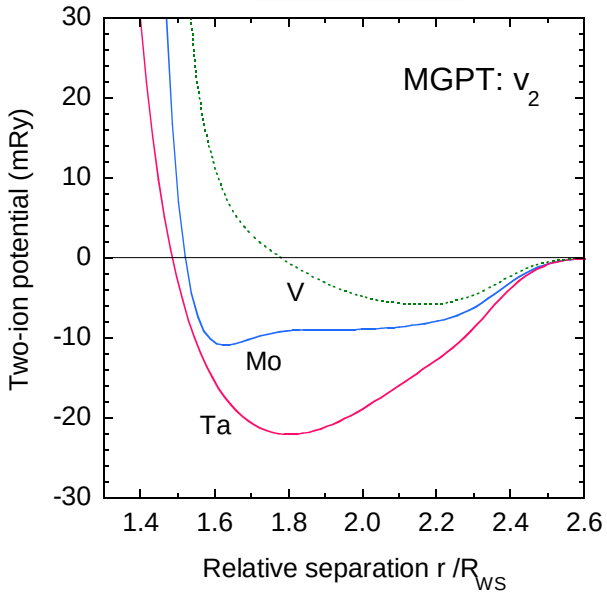

Three-ion

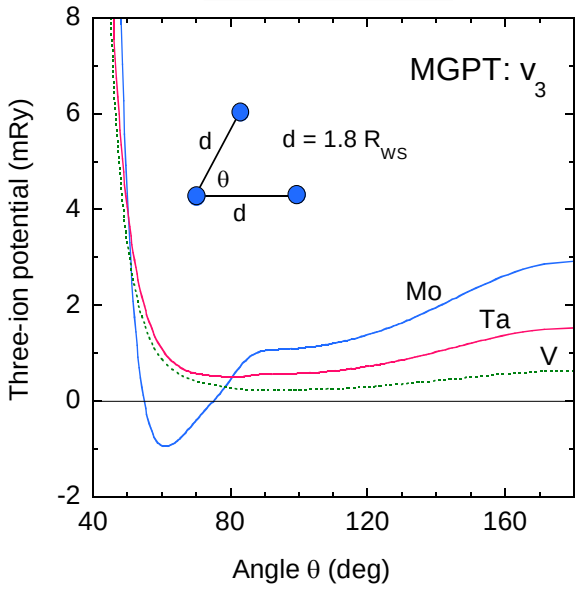

Four-ion

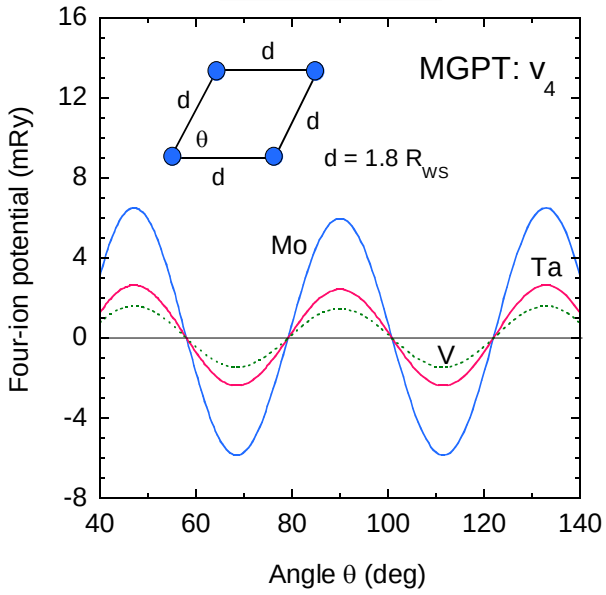

- **Pressure ranges treated:**
  - Ta to 1000 GPa
  - Mo to 400 GPa
  - V to 230 GPa

Volume-dependent MGPT potentials available over wide pressure ranges

Transition-metal MGPT potentials have been widely applied to thermodynamic and mechanical properties

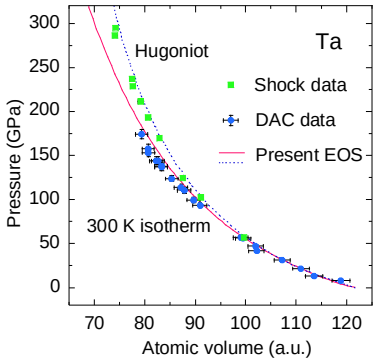

Multi-phase EOS

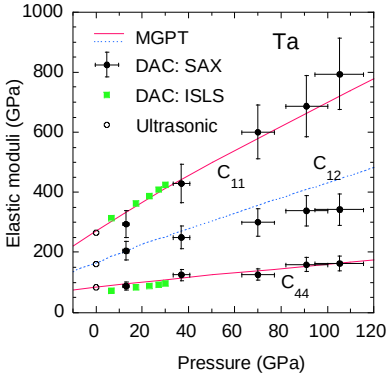

High-P,T elastic moduli

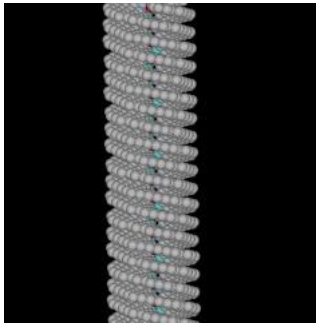

Dislocation structure and mobility

- **Structural and thermo-dynamic properties:**
  - **phase transitions**
  - **phonons**
  - **high-pressure melting**
  - **multiphase EOS**
  - **rapid solidification**
  - **thermoelasticity**
- **Defects and mechanical properties:**
  - **high-pressure elastic moduli**
  - **vacancy, self-interstitial formation and migration**
  - **grain boundary structure**
  - **dislocation structure and mobility**
  - **multiscale modeling of plasticity and strength**

High-P melt

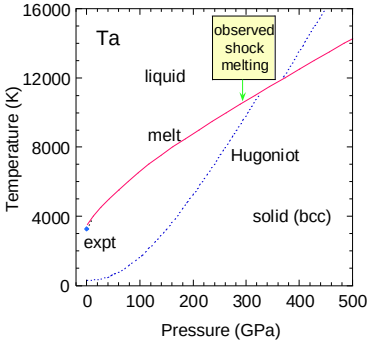

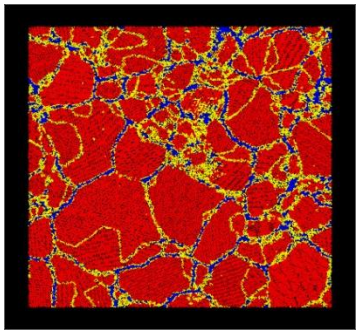

Rapid solid-ification

Grain boundary atomic structure

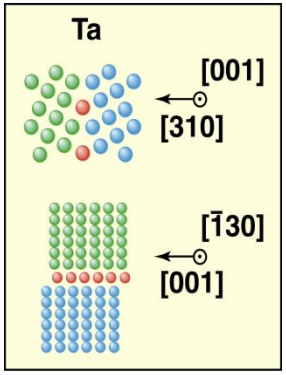

Reviews: JPCM **14**, 2825 (2002); JMR **21**, 563 (2006); *Dislocations in Solids* **16**, 1 (2010)

Structural phase stability and high-pressure phase transitions in central *d*-transition metals

- **Primary trends**
  - structure controlled by *d*-band filling: hcp – bcc – hcp sequence
  - *sp* → *d* electron transfer under pressure
  - high-*P* transition to structure on immediate right:

    IVB metals → bcc
    VB metals remain stable in bcc
    VIB metals → hcp

IVB	VB	VIB	VIIB
hcp Ti	bcc V	bcc Cr	hcp (Mn)
Zr	Nb	Mo	Tc
Hf	Ta	W	Re

- **Secondary trends**
  - driven by details of electronic structure
  - IVB metals: intermediate ω phase, so high-*P* sequence is hcp → ω → bcc
  - bcc metals: competitive A15 structure, especially in Ta and W at low *P*
    possibly stable ω phase in Ta at high *P,T*
  - VB metals: Fermi-surface driven elastic anomalies: bcc → rhom → bcc in V

Structural phase stability in Mo

- **MGPT structural energies and high-pressure trends:**
  - good description ***without* constraint:** v_4 essential to correct physics
  - bcc → hcp predicted beyond 400 GPa: sign of v_4 changes
  - systematic improvement possible: beyond canonical bands and/or beyond v_4

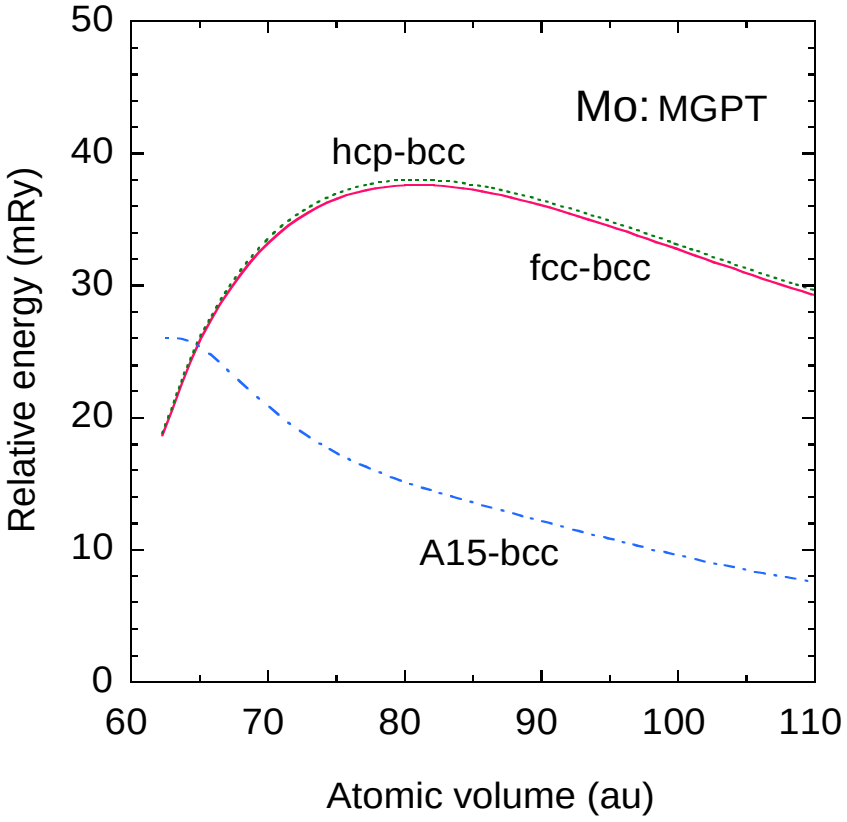

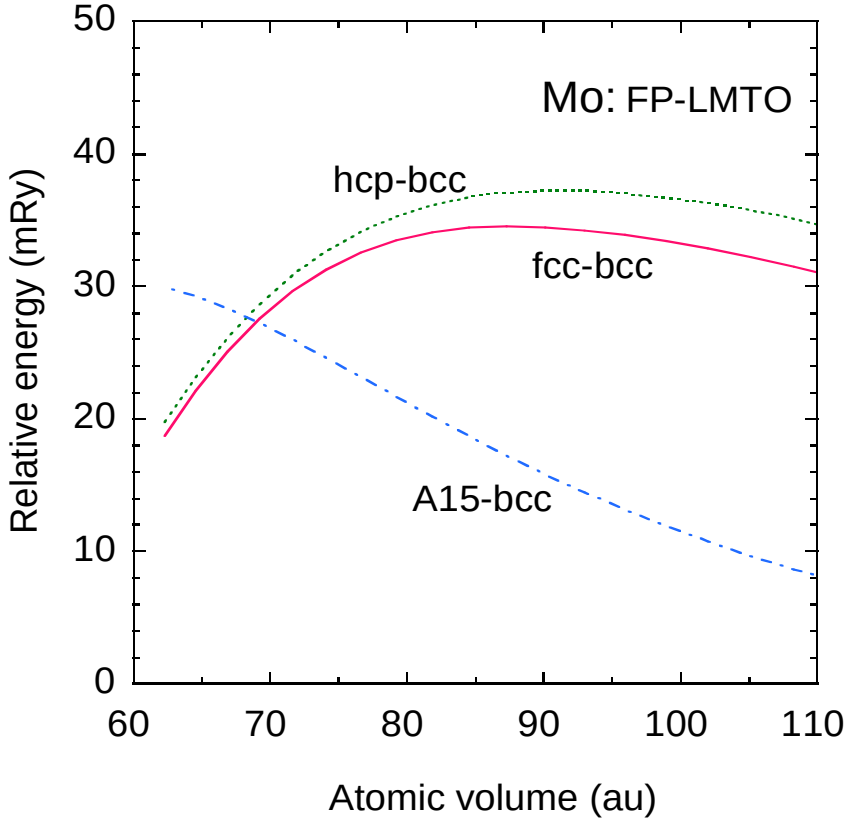

Elastic anomalies and bcc → rhom transition in V

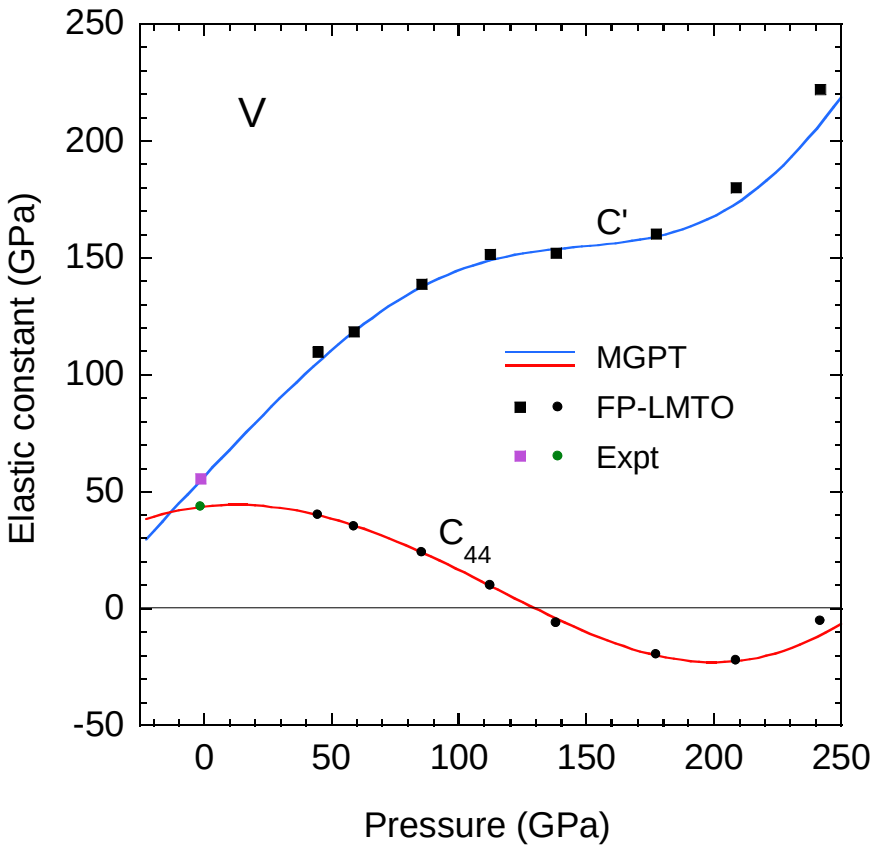

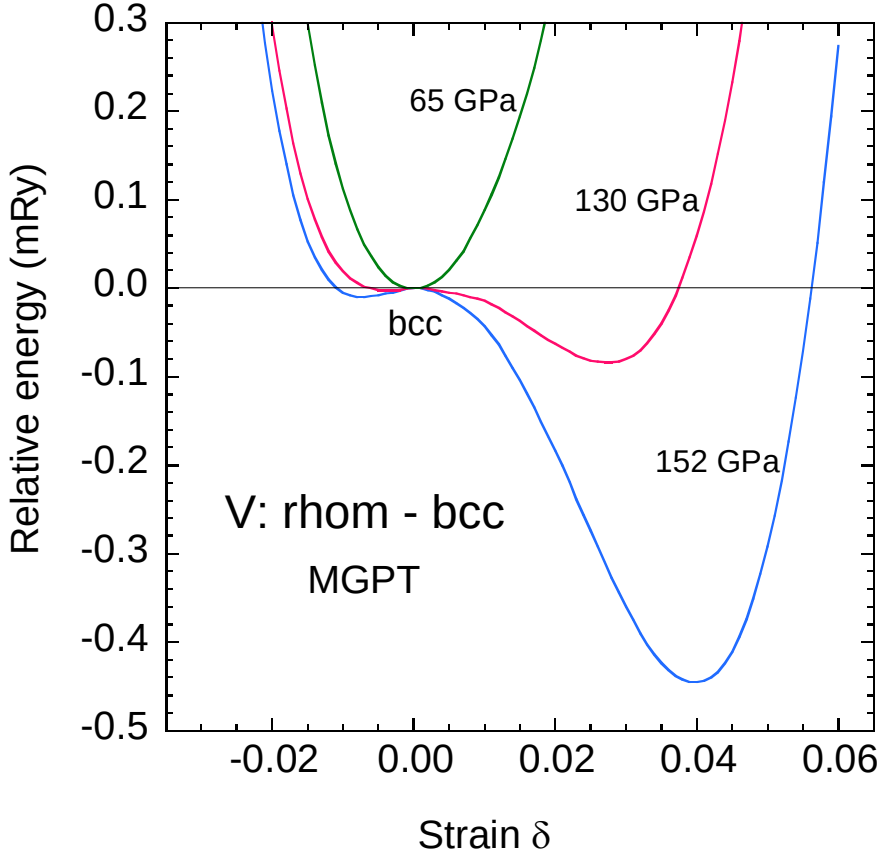

- **bcc → rhom transition seen in DAC at 69 GPa:** Ding *et al.*, *PRL* **98**, 085502 (2007)
- **MGPT potentials capture this behavior through elastic moduli C_{ij} :**
  - softening of C_{44} is precursor to transition
  - transition onset near 65 GPa: T_2[110] zone-boundary phonon becomes imaginary

Multiphase equation of state and melt: Ta prototype

$$A^{\alpha}(\Omega,T) = E_0(\Omega) + A^{\alpha}_{ion}(\Omega,T) + A^{\alpha}_{el}(\Omega,T) \qquad \alpha = bcc, (A15, \omega, \cdots), liquid$$

free energy: cold ion-thermal electron-thermal

- **Cold and electron-thermal components: FP-LMTO coupled to MGPT**
  - T = 0 properties: E_0 , P_0 ; C_{ij} , …
    constraints for MGPT potentials
  - finite temperature: A_{el} , P_{el} , E_{el} , S_{el}
    high-T structure from MD/MGPT

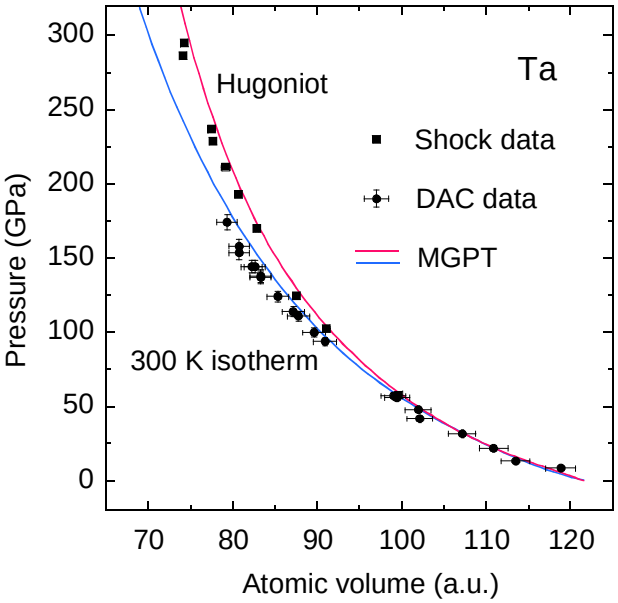

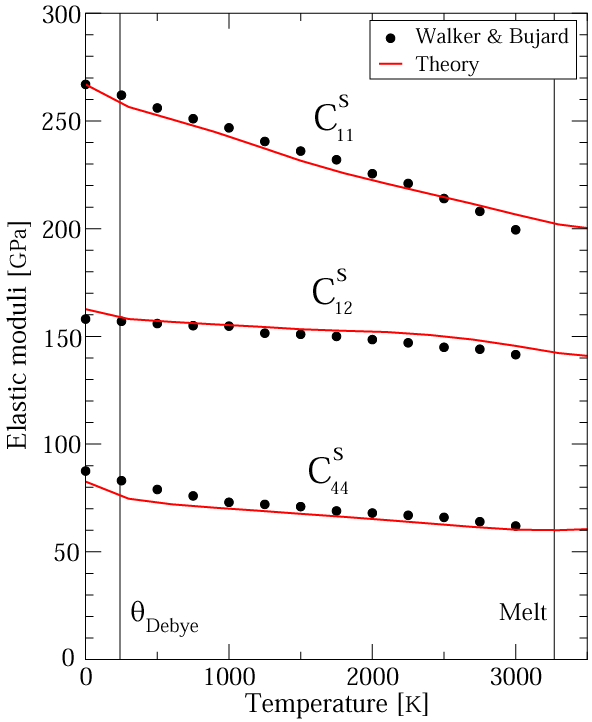

- **Ion-thermal components: MGPT**
  - lattice/liquid thermal properties: A_{ion} , P_{ion} , E_{ion} , S_{ion}
  - MD simulation in high-T solid and liquid

- **Extension to *thermoelasticity*, and recently *polymorphism*, in high-*P,T* solid**

High-pressure Ta melt curve and shock melting

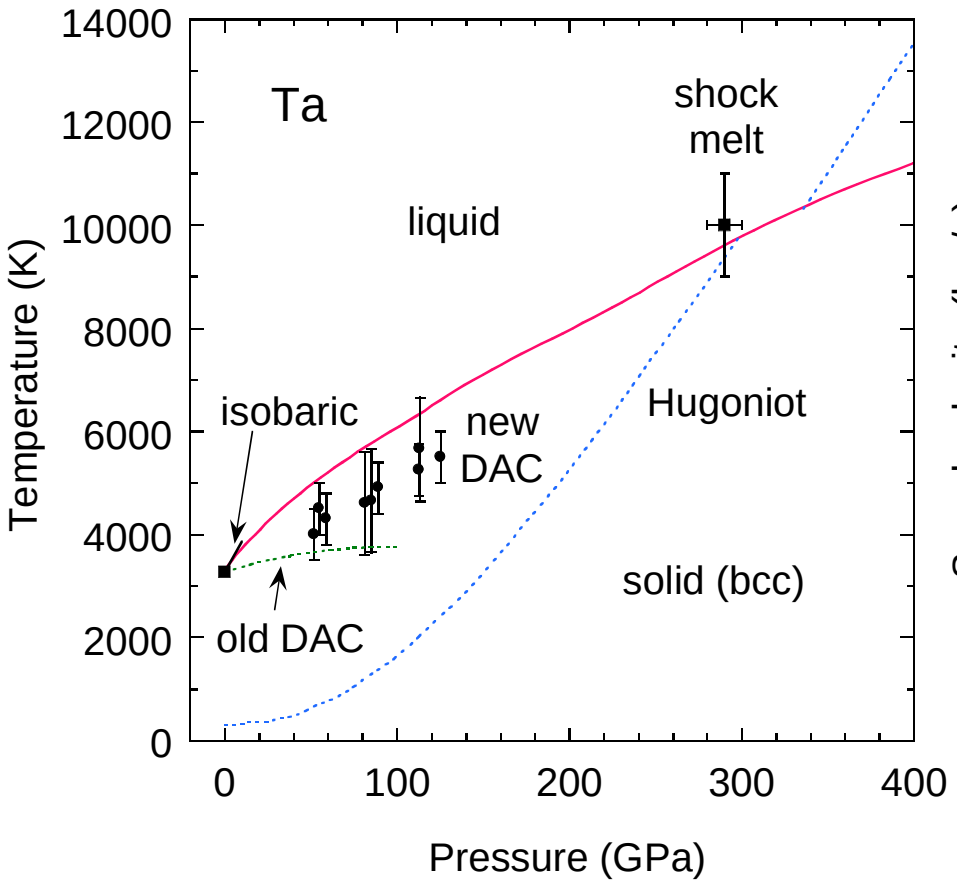

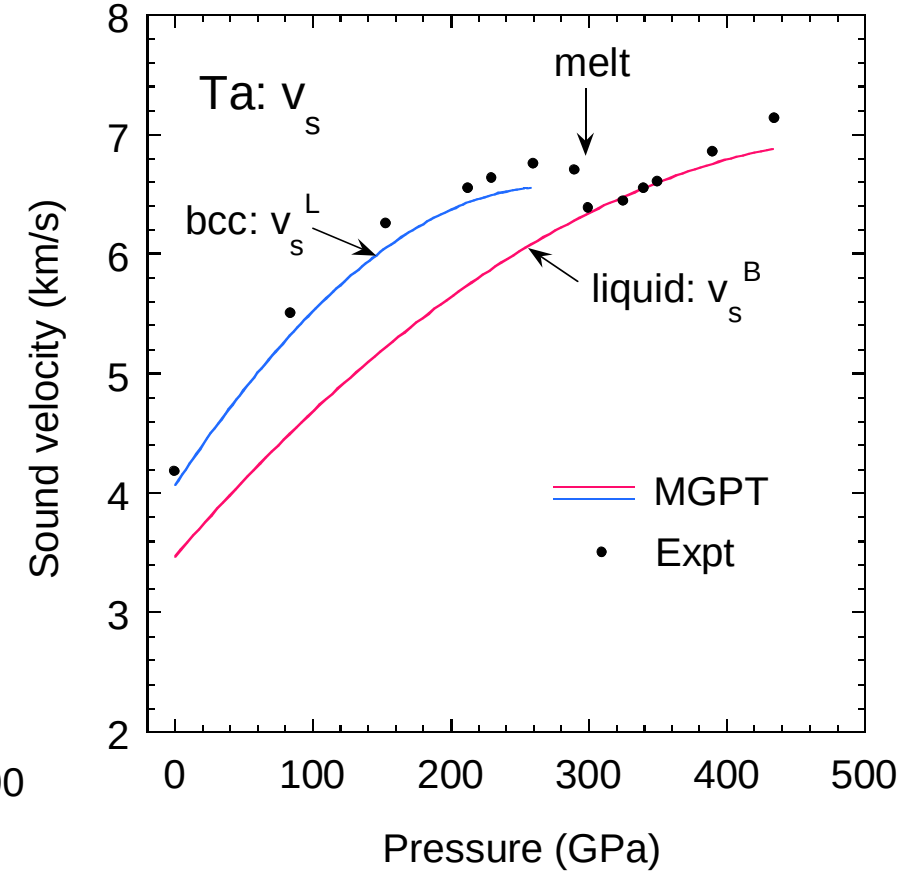

Predicted melt curve agrees with shock and isobaric data, and there is improved agreement with new DAC data: *PRL* 104, 255701 (2010)

Structural disorder of bcc in Ta under shear loading

- MD/MGPT simulations of partial disorder of bcc structure at high *T*
  - Dislocation-free plastic flow on {110} planes matches original DAC “melt”

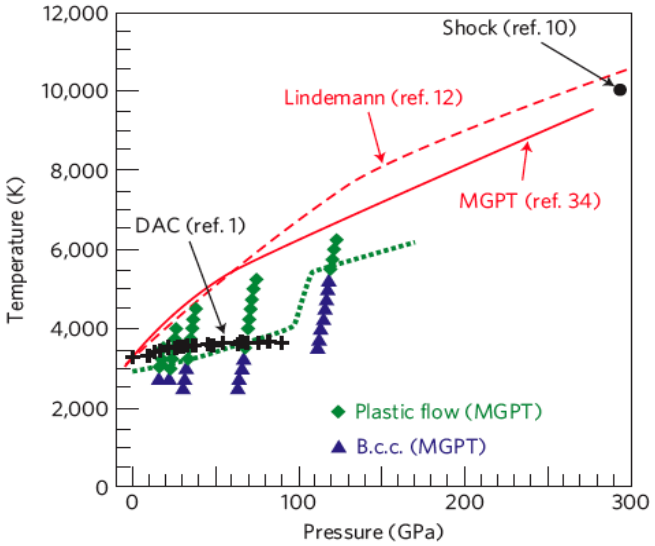

- Possible link to newly discovered polymorphism: Burakovsky *et al*., *PRL* **104**, 255702 (2010)

Planar projections of Ta atomic coordinates (P = 30 GPa)

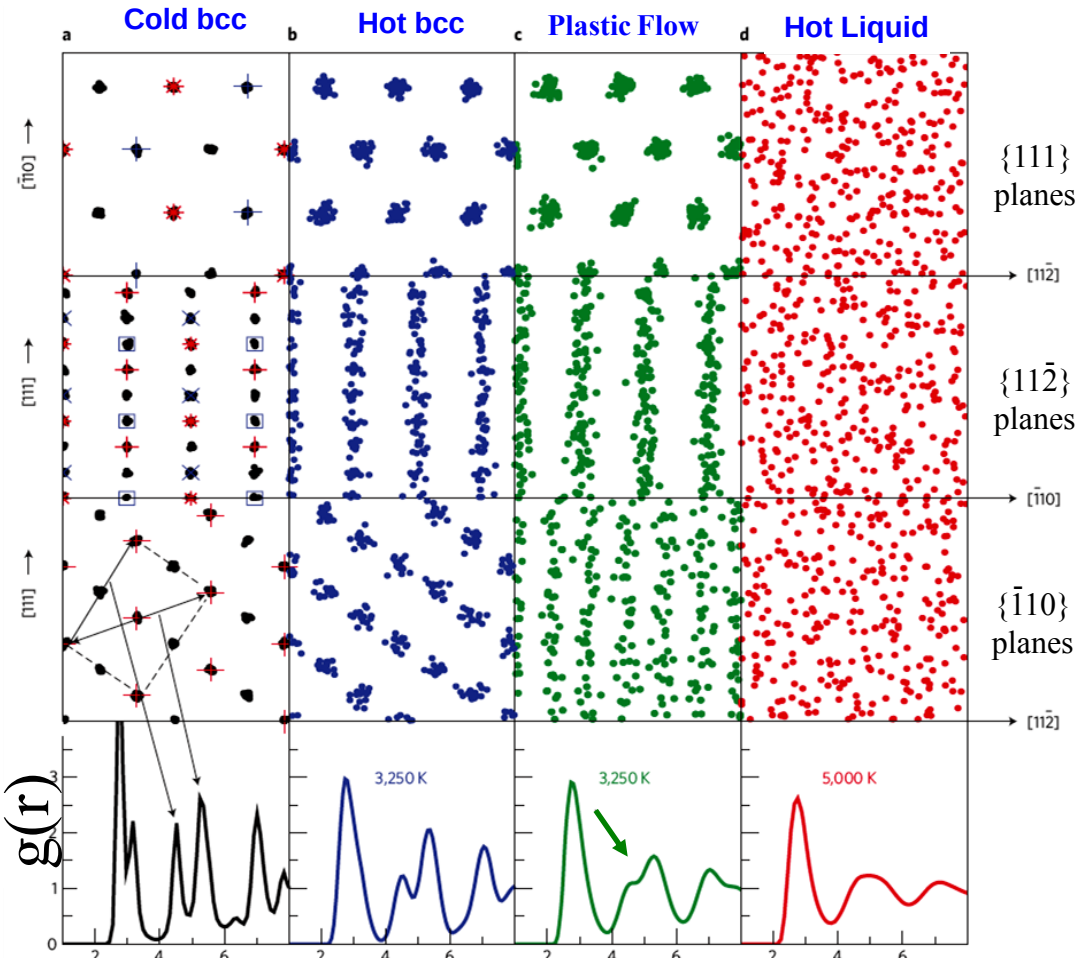

Wu *et al*., Nature Materials **8**, 223 (2009)

Accurate atomistic simulations of dislocation properties in bcc transition metals

- Core structure and its pressure dependence

a/2<111> screw dislocation

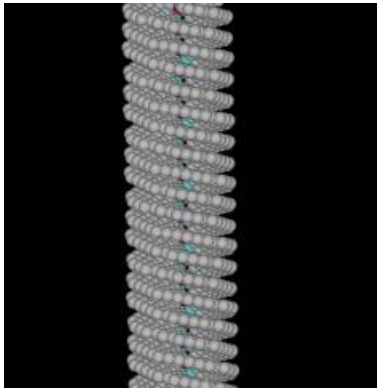

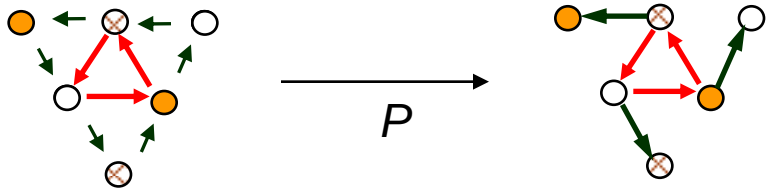

non-degenerate, isotropic

degenerate, polarized

bcc Ta

$P = 0$

$P = 1000$ GPa

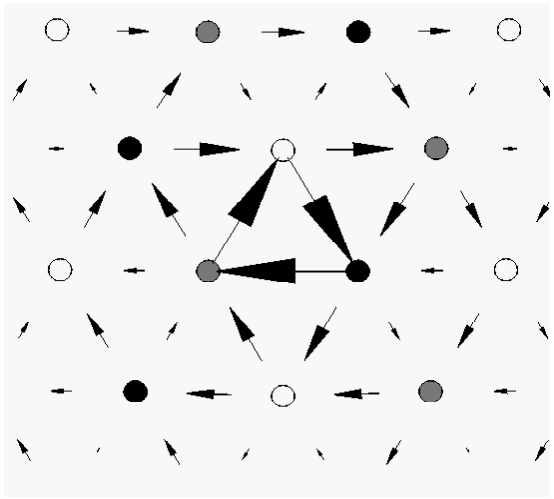

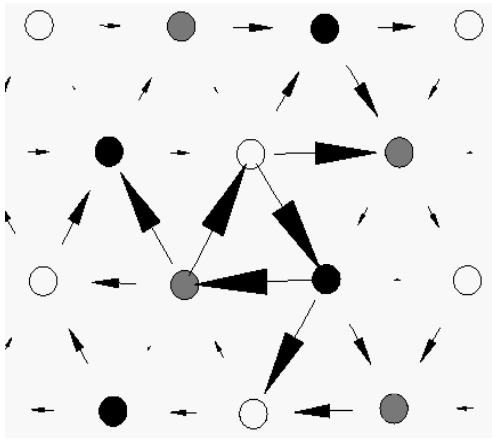

Current consensus view near ambient

But… pressure sensitive core

- Peierls stress τ_P and orientation dependence
- Kink and kink-pair energetics, including stress-dependent activation enthalpy $\Delta H(\tau)$
- Pressure scaling of τ_P and ΔH
- Dynamic simulations of structure and mobility

Linking atomistics to microscale dislocation dynamics (DD) simulations

- Screw dislocations move via thermally activated kinks

Left kink of a/2<111> kink pair

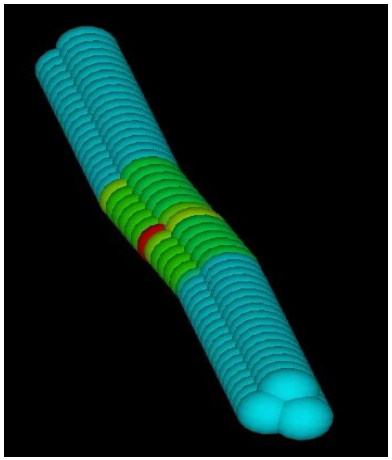

$$v_{screw}(\tau) \propto \exp[-\Delta H(\tau)/k_B T]$$

- Stress-dependent activation enthalpy ΔH
  - controls dislocation mobility and is key input into DD simulations of yield stress
  - orientation dependence and pressure scaling through $\Delta H\ (0)$ and τ_P

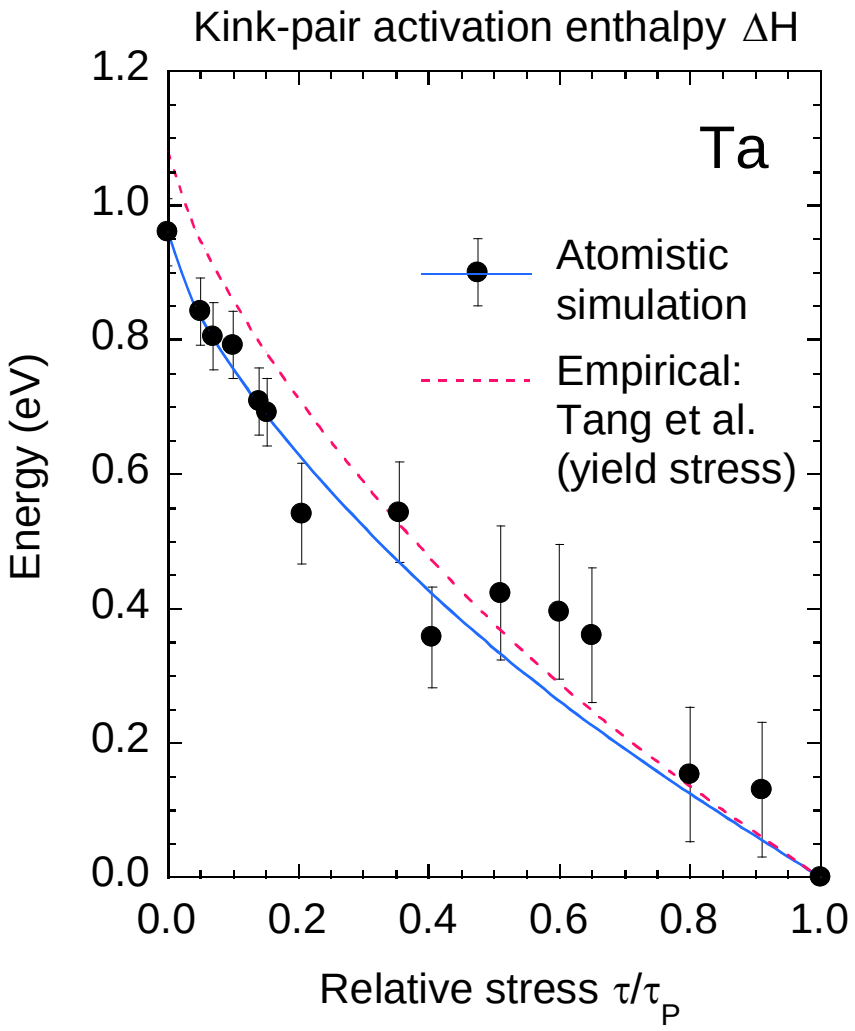

Extended to high pressure for DD yield stress simulations

Atomistically informed DD simulations of single-crystal yield stress in bcc metals

- Atomistic calculations of kink-pair enthalpy fitted to analytic form needed for DD:

$$\Delta H(\tau) = \Delta H(0)[1-(\tau/\tau_P)^p]^q$$

for each pressure considered

- Additional needed quantities τ_P, ν_D, b etc. are also imported from atomistic calculations

- In Ta, τ_P is *scaled down* by about a factor of two to account for ambient-pressure overestimate

- Similar DD simulations have also been done for Mo, but *without* the need for τ_P scaling

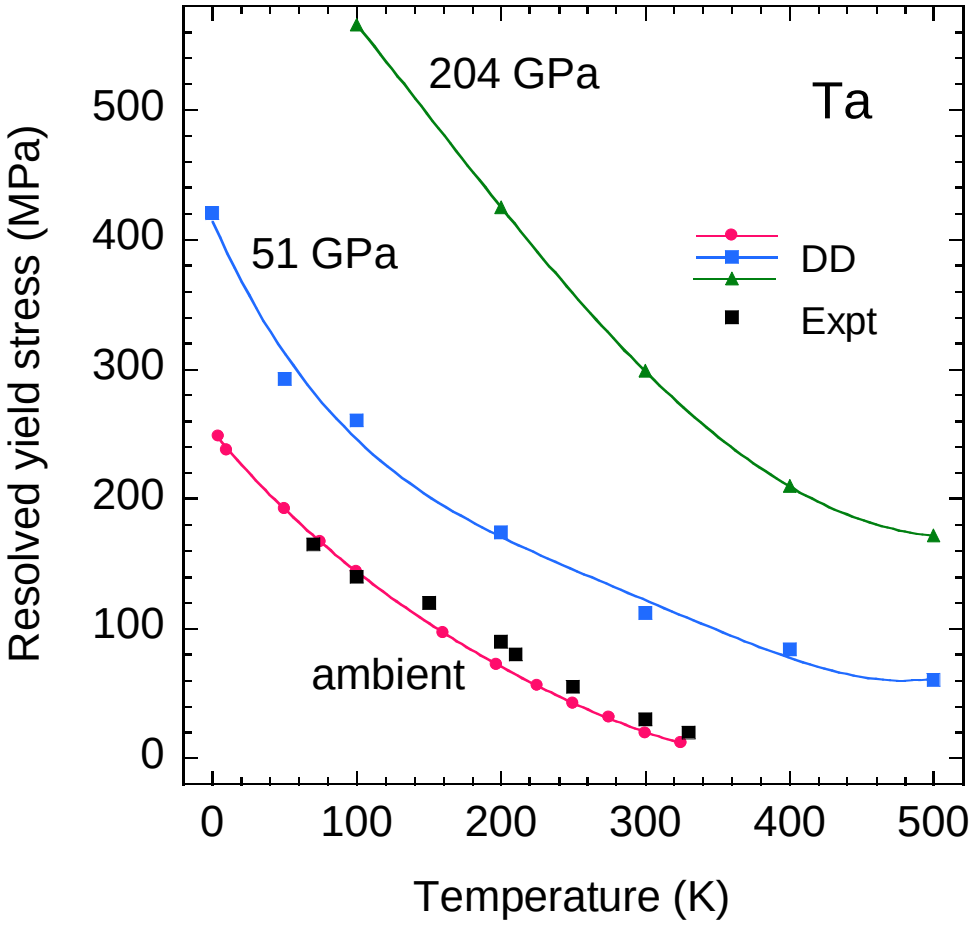

Yang *et al*., *Dislocations in Solids* **16**, 1 (2010)

Matrix MGPT for *f* electrons, non-canonical bands and high speed

- **On-the-fly matrix multiplication of angular functions *P, L, M* :**

$$P \propto Tr(\hat{H}_{ij}\hat{H}_{ji}\hat{H}_{ik}\hat{H}_{ki}) \qquad L \propto Tr(\hat{H}_{ij}\hat{H}_{jk}\hat{H}_{ki}) \qquad M \propto Tr(\hat{H}_{ij}\hat{H}_{jk}\hat{H}_{kl}\hat{H}_{li})$$

- **Canonical bands: *d* → *f* extension for actinide metals**

d states: $\ell = 2$	α_0: α_1: α_2
$p = 2\ell + 1 = 5$	6: -4: 1

→

f states: $\ell = 3$	α_0: α_1: α_2: α_3
$p = 2\ell + 1 = 7$	20: -15: 6: -1

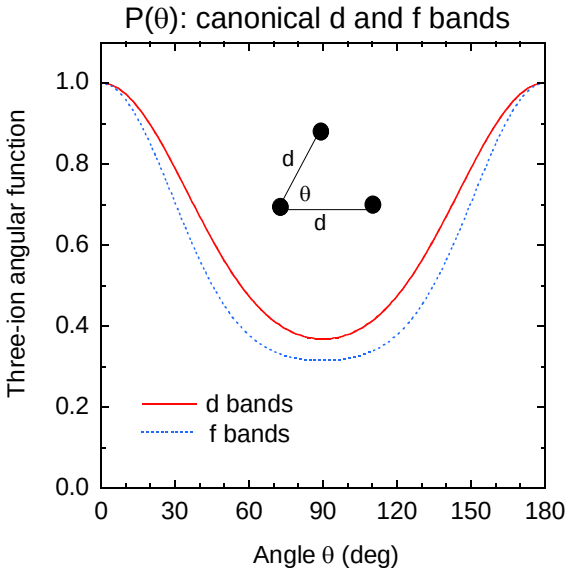

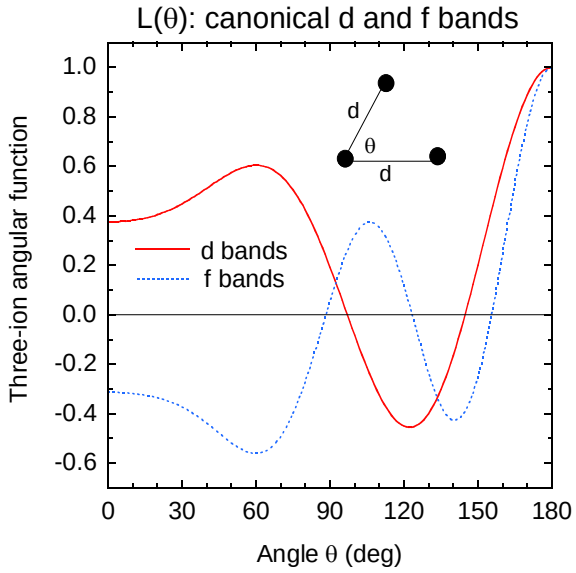

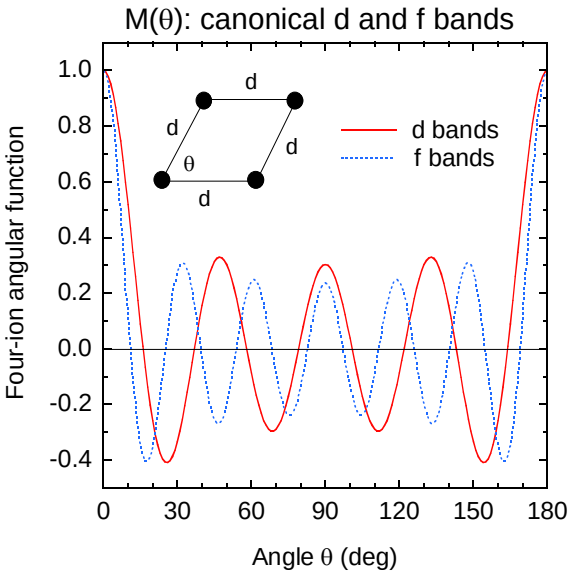

- **Non-canonical bands:** p and α_m become variable input parameters
- **Fast algorithms:** analytic forces with 10-fold speed increase over standard MGPT

Non-canonical bands for improved accuracy

- Non-canonical bands permit an improved description of the underlying electronic structure at *no* additional computational cost

- For *d* bands, there are two additional MGPT parameters:

$$c_0 = \alpha_0 / \alpha_2 \qquad c_1 = \alpha_1 / \alpha_2$$

  which can be volume dependent

- For a given electron temperature a single set of parameters c_0, c_1 improve *all* phonons frequencies at *all* volumes

H-point bcc phonon:

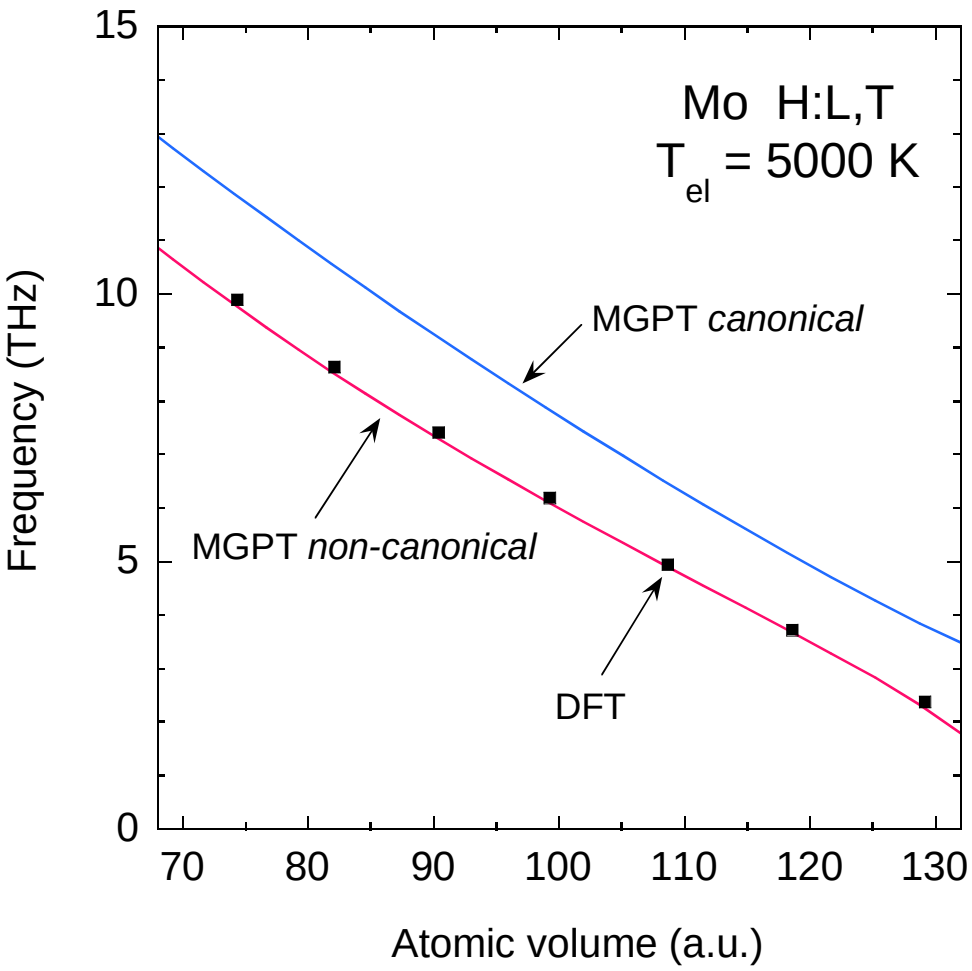

Inclusion of *sp-d* hybridization in MGPT formalism is important for series-end transition metals

In full GPT: $v_2 = v_2^{hc} + v_2^{sp} + v_2^{sp-d} + v_2^{d}$

$$v_3 = v_3^{sp-d} + v_3^{d}$$

$$v_4 = v_4^{sp-d} + v_4^{d}$$

In MGPT:

- model v_n^d via *canonical* or *non-canonical d* bands in usual way
- introduce screened effective hybridization potential:

$$v_{2-eff}^{sp-d} = v_2^{sp-d} + \left\langle v_3^{sp-d} \right\rangle + \left\langle v_4^{sp-d} \right\rangle + \cdots$$
$$= v_2^{sp-d} f_{scr}$$

- potential range reduced by factor of two
- successfully applied to Ni at v_2 level

MGPT pair potentials for Ni with *sp-d* hybridization

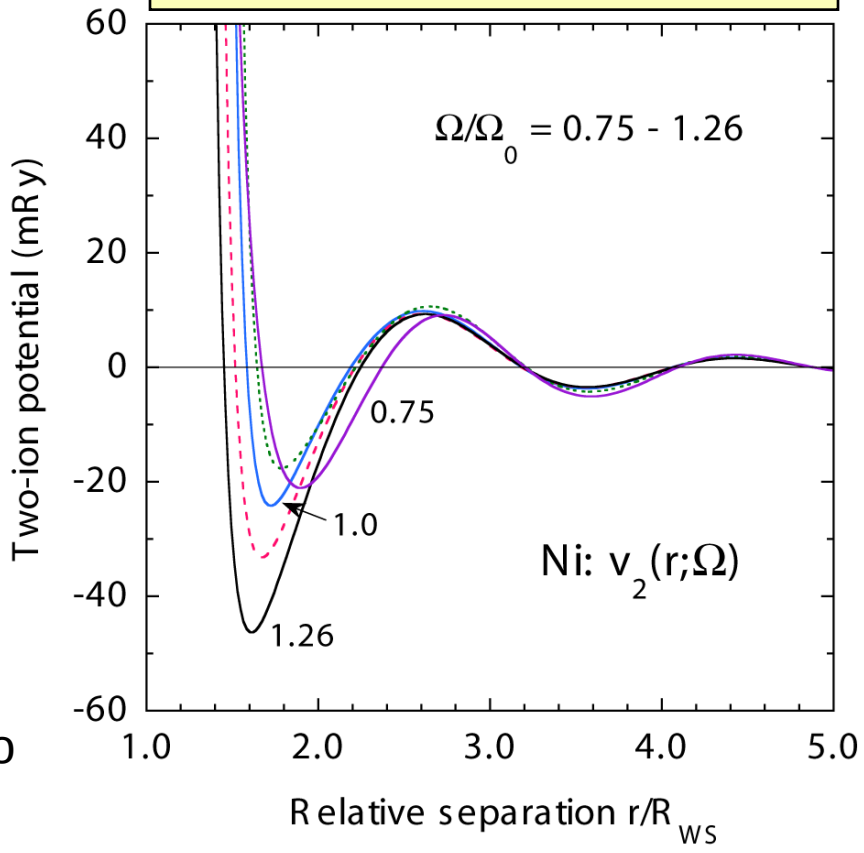

Ni generalized stacking fault (GSF) energies at ambient pressure

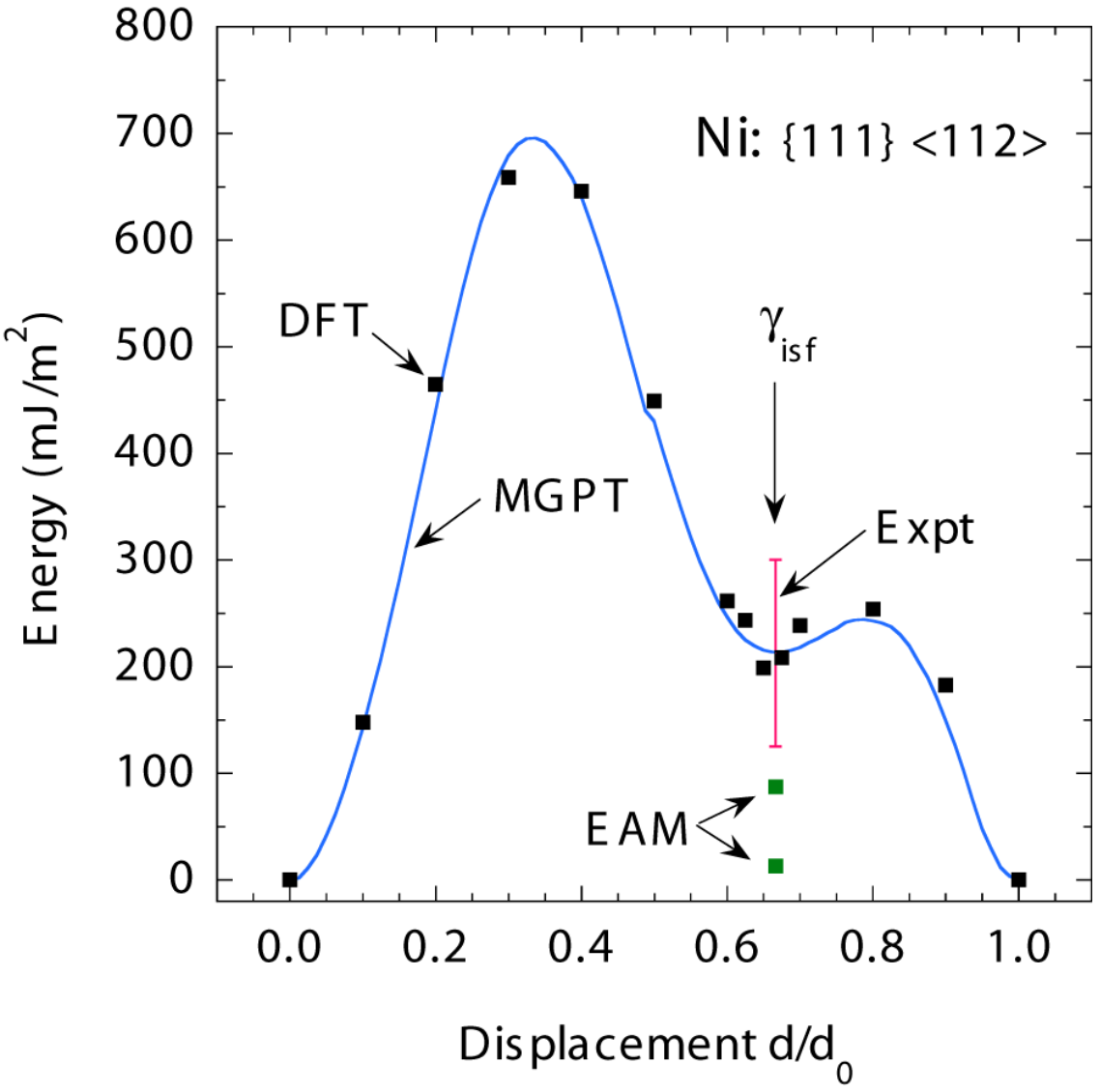

- MGPT closely matches DFT over the entire {111}<112> boundary
- Intrinsic stacking fault energy γ_{isf} calculated in experimental range
- In contrast, short-range EAM potentials under-estimate γ_{isf}
- Ni MD/MGPT simulations of dynamic fracture in progress

Temperature-dependent MGPT potentials for strong-coupling transition metals: Mo prototype

- **Use free-energy functional at finite *electron temperature*:** $T_{el} = T_{ion} = T$

$$A_{tot}(R_1,\ldots,R_N) = NA_{vol}(\Omega,T) + \frac{1}{2}{\sum_{i,j}}' v_2(ij;\Omega,T) + \frac{1}{6}{\sum_{i,j,k}}' v_3(ijk;\Omega,T) + \frac{1}{24}{\sum_{i,j,k,l}}' v_4(ijkl;\Omega,T)$$

volume radial forces angular forces

  - subsumes electron thermal A_{el} and provides T-dependent forces for MD

- **Density of states (DOS), structural and elastic properties sensitive to T_{el}**

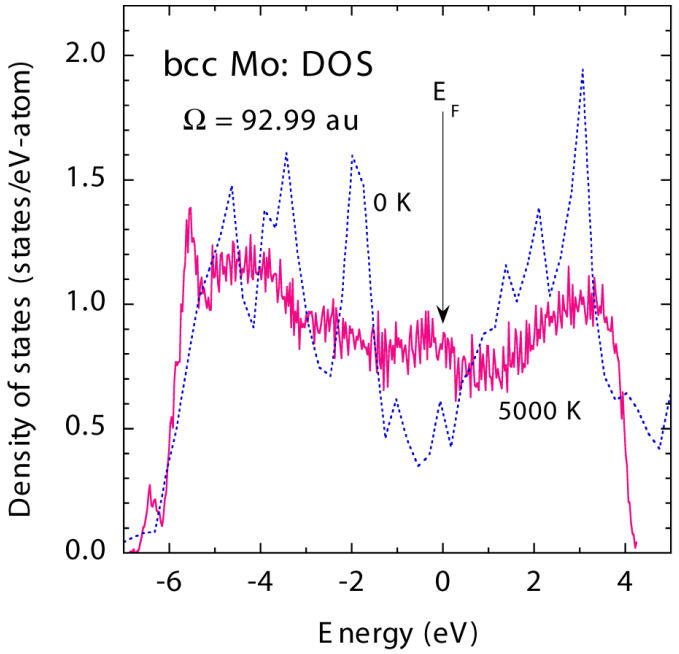

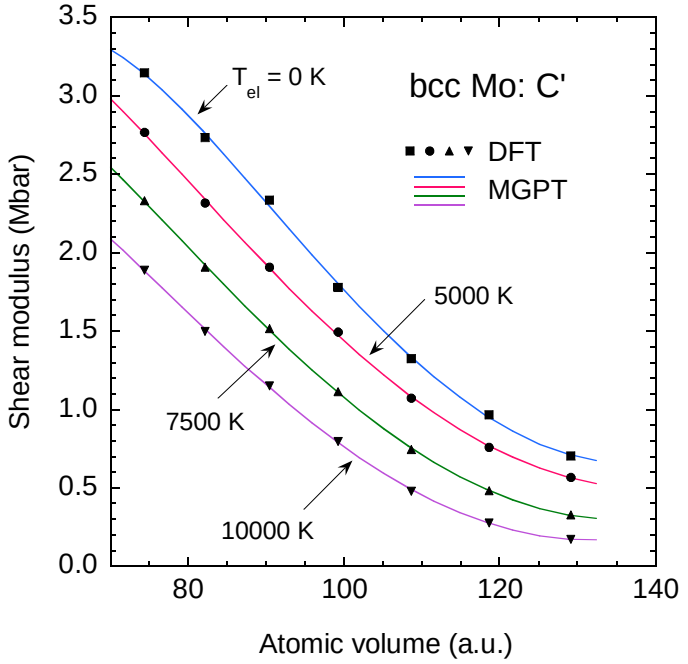

Melting in Mo requires temperature-dependent MGPT potentials

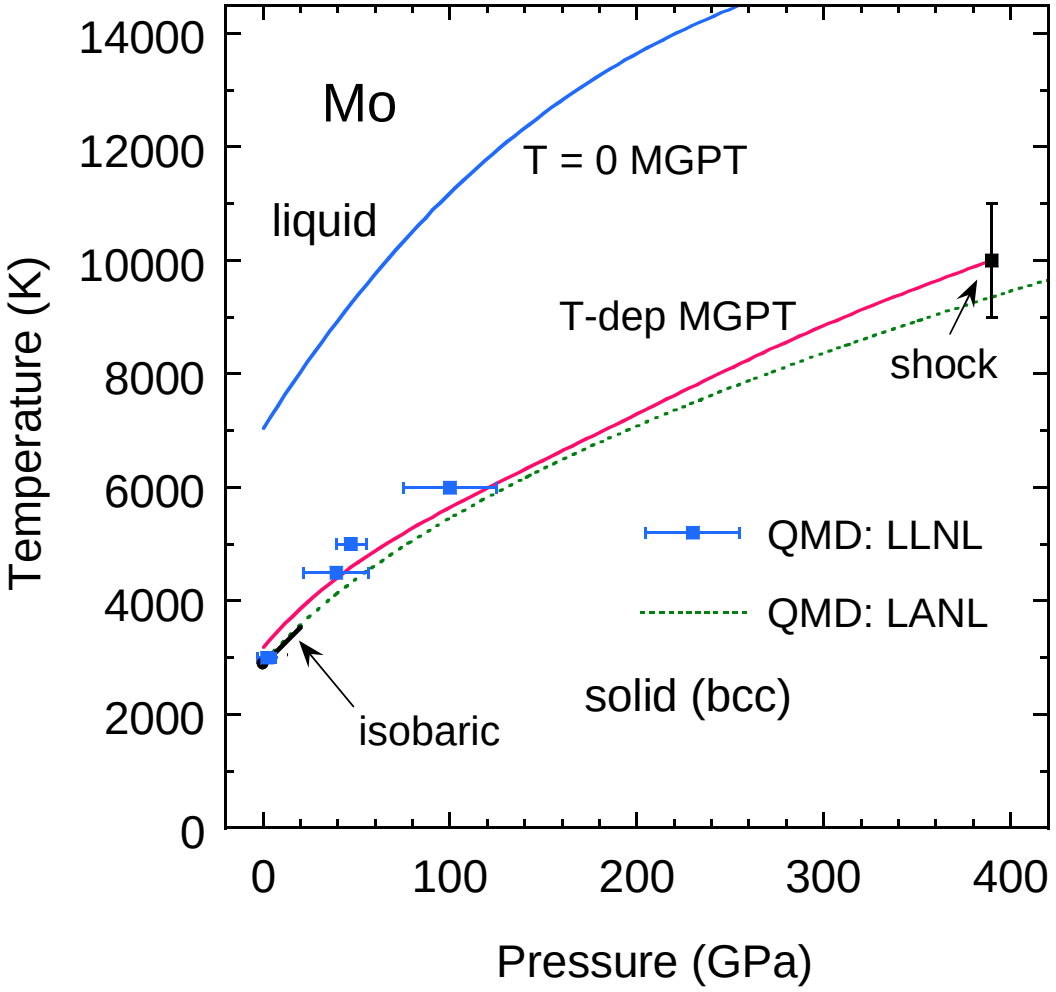

- T = 0 MGPT potentials overestimate melt T_m by factor of two
- T-dep MGPT melt in good agreement with isobaric and shock data as well as with first-principles QMD simulations
- Polymorphism in high-P,T solid currently being studied with T-dependent potentials